Protein tyrosine phosphatase TbPTP1

Protein tyrosine phosphatase *Tb*PTP1: a molecular switch controlling life cycle differentiation in trypanosomes

Balázs Szöőr,[1,2] Jude Wilson,[2] Helen McElhinney,[1,2] Lydia Tabernero,[2] and Keith R. Matthews[1,2]

[1]Institute of Immunology and Infection Research, University of Edinburgh, Edinburgh EH9 3JT, Scotland, UK
[2]Faculty of Life Sciences, University of Manchester, Manchester M13 9PT, England, UK

Differentiation in African trypanosomes (*Trypanosoma brucei*) entails passage between a mammalian host, where parasites exist as a proliferative slender form or a G0-arrested stumpy form, and the tsetse fly. Stumpy forms arise at the peak of each parasitaemia and are committed to differentiation to procyclic forms that inhabit the tsetse midgut. We have identified a protein tyrosine phosphatase (*Tb*PTP1) that inhibits trypanosome differentiation. Consistent with a tyrosine phosphatase, recombinant *Tb*PTP1 exhibits the anticipated substrate and inhibitor profile, and its activity is impaired by reversible oxidation. *Tb*PTP1 inactivation in monomorphic bloodstream trypanosomes by RNA interference or pharmacological inhibition triggers spontaneous differentiation to procyclic forms in a subset of committed cells. Consistent with this observation, homogeneous populations of stumpy forms synchronously differentiate to procyclic forms when tyrosine phosphatase activity is inhibited. Our data invoke a new model for trypanosome development in which differentiation to procyclic forms is prevented in the bloodstream by tyrosine dephosphorylation. It may be possible to use PTP1B inhibitors to block trypanosomatid transmission.

Introduction

African sleeping sickness threatens >60 million people in sub-Saharan Africa, resulting in >70,000 deaths per year, and additional impact is felt through its effects on livestock. The disease is always fatal if untreated, and existing drugs are unacceptably toxic and often require hospitalization (Barrett et al., 2003). With outdated existing drugs, new targets for drug development are urgently needed. This search is being aided by a better understanding of the biology of the causative agent, *Trypanosoma brucei* spp.

The life cycle of *T. brucei* is divided between a mammalian host and the tsetse fly (Matthews, 2005). In mammals, the parasite population consists of proliferative slender cells and nonproliferating stumpy forms, which are arrested in G1/G0 (Matthews et al., 2004). The transition between these forms occurs in response to a parasite-derived signal in the bloodstream (Vassella et al., 1997), resulting in an accumulation of stumpy forms. This optimizes parasite transmissibility because stumpy forms are preadapted for uptake into the tsetse fly (Engstler and Boshart, 2004). In particular, they have upregulated certain metabolic activities in preparation for life in the fly and are more resistant to proteolytic attack and pH fluctuations (Sbicego et al., 1999; Nolan et al., 2000). In the tsetse, stumpy forms differentiate to procyclic forms, a transition that can be efficiently reproduced in culture by cis aconitate and a reduction of temperature (Ziegelbauer and Overath, 1990). Once stimulated to differentiate, stumpy forms embark on a precisely programmed developmental pathway involving changes in cell morphology, metabolic activity, surface antigen expression, and gene expression. Importantly, the generation of stumpy forms in the bloodstream represents an irreversible commitment to differentiate; stumpy forms not taken up in a fly blood meal ultimately degenerate in the bloodstream (Turner et al., 1995).

In higher eukaryotes, tyrosine phosphorylation is a well-characterized mechanism for regulating cell growth and differentiation, as well as many other aspects of cell life (Neel and Tonks, 1997; Tonks, 2003). However, less is known about tyrosine phosphorylation events in lower eukaryotes and prokaryotes. For example, in bacteria, protein tyrosine phosphorylation is a rare occurrence and yet tyrosine phosphatases are essential

Correspondence to Lydia Tabernero: lydia.tabernero@man.ac.uk; or Keith R. Matthews: keith.matthews@ed.ac.uk

Abbreviations used in this paper: BZ3, 3-(3,5-Dibromo-4-hydroxy-benzoyl)-2-ethyl-benzofuran-6-sulfonicacid-(4-(thiazol-2-ylsulfamyl)-phenyl)-amide; EGFR, EGF receptor; pNPP, *p*-nitrophenylphosphate.

The online version of this article contains supplemental material.

The Journal of Cell Biology, Vol. 175, No. 2, October 23, 2006 293–303
http://www.jcb.org/cgi/doi/10.1083/jcb.200605090

for infection and survival of pathogenic species like *Salmonella*, *Yersinia*, or *Mycobacterium* (Black et al., 2000; Lin et al., 2003; Singh et al., 2003). Kinetoplastid parasites such as *Trypanosoma* spp. and *Leishmania* spp. occupy an interesting evolutionary niche, being unicellular organisms and among the most diverged representatives of the eukaryotic world. Although intracellular signaling events have not yet been described in detail for these organisms, it is likely that tyrosine phosphorylation will also play a role in cellular processes as in higher eukaryotes. Supporting this, there is evidence that several proteins are phosphorylated on tyrosine residues in kinetoplastids (Parsons et al., 1991; Cool and Blum, 1993) presumably through the activity of dual-specificity protein kinases, as kinetoplastid genomes do not encode any recognizable tyrosine-specific kinases (Parsons et al., 2005). Tyrosine phosphatase activity also shows marked differences among different life cycle stages in both *T. brucei* and *T. cruzi* (Bakalara et al., 1995a).

From the precedent in higher eukaryotes, it is likely that phosphotyrosine phosphatases will be also relevant in the control of cell growth and development in kinetoplastids. Supporting this idea, it was recently reported that the heterologous expression of the human PTP1B gene in *Leishmania*, together with the inhibition of tyrosine kinases, promoted partial differentiation from promastigote to amastigote forms (Nascimento et al., 2003). Here, we demonstrate that the activity of a *T. brucei* protein tyrosine phosphatase, *Tb*PTP1, exhibits a pivotal function in parasite differentiation. Biochemical characterization of the enzyme demonstrates that it is a tyrosine-specific phosphatase whose enzymatic activity is regulated by pH and changes in its oxidation state. Importantly, when *Tb*PTP1 activity is inhibited by RNAi or biochemically, differentiation to procyclic forms occurs spontaneously in the absence of any exogenous trigger. This response is restricted to a subset of bloodstream cells, which we propose are those already committed to differentiation. Supporting this, tyrosine phosphatase inhibition in a homogeneous population of stumpy forms triggers synchronous, efficient, and complete differentiation to proliferative procyclic forms. These data reveal that a tyrosine phosphatase activity is a key molecular regulator of the initiation of trypanosome differentiation, providing a potential pharmacological target to restrict parasite transmissibility and virulence.

Results

Identification and expression profile of *Tb*PTP1

To identify molecules implicated in the differentiation competence of bloodstream stumpy forms, we searched the *T. brucei* genome database for molecules that define G1/G0 arrest in other organisms. This revealed a 595-bp fragment with limited sequence similarity to the protein tyrosine phosphatase PTPROt (Aguiar et al., 1999). PTPROt was first identified in mammalian lymphoid organs and is up-regulated in quiescent B cells. The intact *T. brucei* gene was then isolated by PCR from cDNA, and the complete gene sequence was determined. This was subsequently verified upon completion of the *T. brucei* genome project. This gene, which we have named *Tb*PTP1 (*T. brucei* phosphotyrosine phosphatase 1), is positioned on chromosome 10 (Tb10.70.0070).

Previous evidence that protein phosphatase activities were differentially regulated during the trypanosome life cycle (Bakalara et al., 1995b) prompted us to examine the developmental mRNA expression profile of *Tb*PTP1 by Northern blotting. Total RNA was prepared from monomorphic bloodstream slender forms, bloodstream stumpy forms, and in vitro–cultured procyclic forms. This revealed that the *Tb*PTP1 mRNA was expressed in all stages examined, although up-regulated in stumpy forms (1.5–3-fold), which was somewhat variable between samples (Fig. 1 A). To relate mRNA expression to that of the protein, an anti-peptide antibody was raised against the sequence N-AMKQKRFGMVQRLEQ-C from the amino acid sequence at position 265–279 in *Tb*PTP1. When reacted against lysates derived from isogenic monomorphic slender and stumpy forms of *T.b. rhodesiense* EATRO 2340 and procyclic forms of *T. brucei* Lister 427, approximately equal expression of *Tb*PTP1 protein was detected. *Tb*PTP1 expression was also analyzed during synchronous differentiation of bloodstream stumpy forms to procyclic forms. This revealed no transient changes in the protein expression levels of *Tb*PTP1 during the events of differentiation (Fig. 1 B). Finally, analysis of the subcellular localization of *Tb*PTP1 by differential detergent extraction revealed that *Tb*PTP1 associated predominantly with the cytoskeletal fraction in bloodstream forms (Fig. 1 C). Although no association with any discrete structure (e.g., the flagellum) could be detected (Fig. S1, available at http://www.jcb.org/cgi/content/full/jcb.200605090/DC1), a cytoskeletal association for *Tb*PTP1 matches the distribution of several tyrosine phosphatases characterized in other organisms (Howard et al., 1993; van Ham et al. 2005). This compartmentalization is believed to contribute to their substrate specificity.

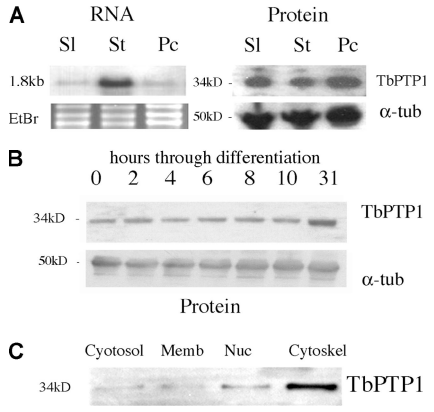

Figure 1. ***Tb*PTP1 is uniformly expressed during the trypanosome life cycle and localizes with the cytoskeletal fraction.** (A) Northern and Western analysis of *Tb*PTP1 levels in slender (Sl), stumpy (St; both *T.b. rhodesiense* EATRO 2340) and procyclic (Pc; *T.b. brucei* s427) cells. Loading controls of ethidium bromide–stained total RNA (for the Northern blot) and α-tubulin (for the Western blot) are shown. (B) Protein expression of *Tb*PTP1 during synchronous differentiation to procyclic forms. (C) Cellular distribution of *Tb*PTP1 in stumpy forms. Cytosolic, membrane, nuclear, and cytoskeletal fractions are shown. *Tb*PTP1 associates with the cytoskeletal fraction. Other cellular markers partition as expected (cPGK, cytosolic; BiP, membrane and cytosolic; and α-tubulin, cytoskeletal and cyotosolic; not depicted).

The *Tb*PTP1 is a member of a trypanosome-specific PTP1 family

The 1.8-kb *Tb*PTP1 mRNA contains an ORF of 921 nucleotides encoding a protein of 306 amino acids with a predicted molecular mass of 34 kD. A predicted PEST sequence region is located between residues 135 and 152 (Fig. 2, underlined). Analysis of the amino acid sequence of *Tb*PTP1 revealed an N-terminal region (43 residues) with no apparent homology to any other protein and a C-terminal region (263 residues) that is homologous to the human protein tyrosine phosphatases PTP1B and PTPROt (24 and 23% identity over the catalytic domain of each molecule, respectively). An extensive search of different trypanosomatid databases, identified orthologues of *Tb*PTP1 in *T. congolense* (*Tcg*PTP1, with 74.1% identity), *T. vivax* (*Tv*PTP1, with 62.0% identity), and *T. cruzi* (*Tc*PTP1, with 61.3% identity). The sequence alignment of these orthologues together with human PTP1B is shown in Fig. 2. When sequence similarity is considered, these values rise to 71–80% between *Tb*PTP1 and trypanosomal PTP1s, compared with 38% to human PTP1B. In contrast, *Leishmania major* has a syntenic gene encoding a predicted tyrosine phophatase less closely related to *Tb*PTP1 (42% similarity; LmjF36.2180).

Previous sequence analysis of human PTPs have led to the identification of 10 conserved motifs, some of which are important in substrate binding and catalysis (Andersen et al., 2001). The trypanosomal PTP1 subfamily contains all the landmark motifs present in classical tyrosine-specific phosphatases (Fig. 2). These include the phospho-Tyr binding motif (Fig. 2, M1); the WPD loop (M8), which contains the catalytic aspartic acid (the general acid in catalysis); the catalytic P-loop or PTP signature motif (V/I)HCSAGXGR (T/S) (M9); and the Q-loop (M10), which is part of the active site in classic PTPs. Motifs 3–7 (M3–M7) are also present in trypanosomal PTP1s with a high percentage of conservation, consistent with their role as structural motifs located in the core of the PTP catalytic domain. In total, 9 of the 10 well-conserved PTP motifs identified in the mammalian enzymes are present in all the examined trypanosome PTP1s, with only the less-conserved motif 2 missing. Instead of motif 2, a trypanosome-specific motif, T1, replaces this structural motif.

Other distinct motifs were also identified in the trypanosomal PTP1s, generating a total of four trypanosome-specific motifs in the catalytic region (Fig. 2, T1–T4). These are as follows: T1 at position 55–63, "LANEXTIYP"; T2 at position 165–167, "EVD"; T3 at position 239–244, "LIGAYA"; and T4 at position 290–295, "RLGV (D/S) (I/V)." In addition, two other motifs have been identified in the precatalytic (Pc) region: PcT1 "R (M/L)QREFXQLQ" at position 20–29 and PcT2 "ENPRXI (D/N)FTTSL" at position 32–43. These precatalytic motifs are well conserved in all members of the *T. brucei* clade (*T. brucei*, *T. congolense*, and *T. vivax*) and less conserved in *T. cruzi*. A BLAST search failed to identify any of these motifs in other proteins, indicating that they are unique to the trypanosomal PTP1 family. We hypothesize that these trypanosome-specific motifs may be relevant to regulation of *Tb*PTP1 or molecular recognition of other cellular targets.

The activity of *Tb*PTP1 is regulated by reversible oxidation in vitro

Having identified *Tb*PTP1 as a putative tyrosine phosphatase, it was important to characterize its enzymatic activity profile and substrate specificity. For this, recombinant protein was produced for the wild-type protein and for two *Tb*PTP1 mutants, one for the putative catalytic cysteine, Cys 229 (in the P-loop) and one for the catalytic Asp 199 (in the WPD loop). The catalytic mutants of *Tb*PTP1 were generated by mutating Cys 229 to serine (C229S) and Asp 199 to alanine (D199A). The wild-type enzyme and mutant enzymes were expressed as His_6-tagged fusions and purified to >95% homogeneity. After removal of the His tag by enterokinase digestion, multiangle

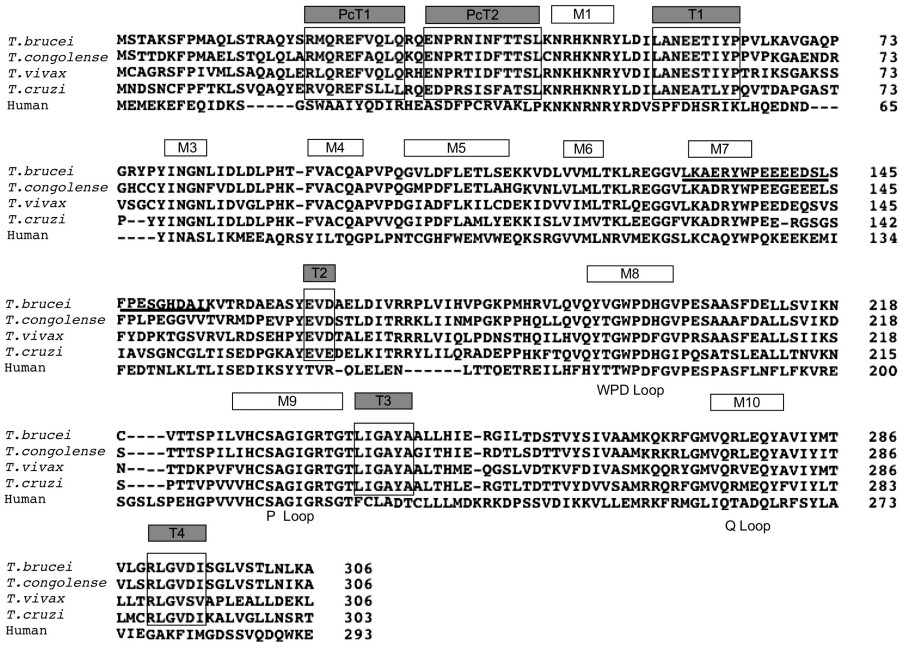

Figure 2. **Alignment of *Tb*PTP1 with orthologue trypanosome PTP1s and the human PTP1B.** The deduced amino acid sequences encoding PTP1 of *T. brucei* (*Tb*10.70.0070), *T. congolense* (congo1301f01.p1k), *T. vivax* (Tviv1180b04.p1k), *T. cruzi* (Tc00.10470535 10187.234), and the human PTP1B (P18031) were aligned using CLUSTAL X (Thompson et al., 1997). The classical PTP motifs are indicated above the sequences in white boxes (M1–M10). The trypanosome-specific motifs are boxed in gray. PcT1 and PcT2 are the precatalytic motifs, and the T1–T4 motifs are conserved in the catalytic region. The predicted PEST sequence is underlined.

light scattering analysis of the enzyme showed that *Tb*PTP1 behaves as a monomeric protein in solution, with a determined mass of 35,140 D.

The phosphatase activities of the purified recombinant wild-type, D199A, and C229S enzymes were assayed using various concentrations of *p*-nitrophenylphosphate (pNPP), a widely used substrate of tyrosine phosphatases. The pH profile analysis of pNPP dephosphorylation demonstrated that the wild-type enzyme has the highest specific activity at pH 6.0 (Fig. 3 A), in agreement with the fact that PTPs in general have optimal enzymatic activities at low pH values. The mutant enzyme D199A showed low activity (5–8% of the wild type), and the C229S mutant enzyme was totally inactive under any assay condition and substrate concentration tested (unpublished data). This confirms our predictions from the sequence analysis and demonstrates that both residues, Cys 229 and Asp 199, are essential in the mechanism of catalysis of *Tb*PTP1, matching their orthologues in mammalian PTPs. Steady-state kinetic analysis of the wild-type enzyme yielded a V_{max} value of 0.12 mM min^{-1} and a k_{cat}/K_m of 3.57 $mM^{-1} \times s^{-1}$ for the dephosphorylation of pNPP. Addition of 2 mM of DTT had a marked effect on the catalytic rate, increasing the V_{max} by threefold and the k_{cat}/K_m by 14-fold (Fig. 3 B and Table S1, available at http://www.jcb.org/cgi/content/full/jcb.200605090/DC1), consistent with previous observations suggesting that the catalytic cysteine needs to be in a reduced state for efficient nucleophilic attack of the substrate (Denu and Tanner, 1998). To investigate whether redox events (Denu and Tanner, 1998; Salmeen et al., 2003; van Montfort et al., 2003) could influence the enzymatic activity of *Tb*PTP1, we performed a time course activity assay using increasing amounts of the oxidizing agent, hydrogen peroxide (H_2O_2). Fig. 3 C shows that after 10 min of incubation, the addition of 0.25 mM H_2O_2 completely inactivated *Tb*PTP1 and 0.025 and 0.1 mM H_2O_2 reduced the enzyme activity by 37 and 58%, respectively. Importantly, the enzymatic activity of the inactive *Tb*PTP1 toward pNPP was completely restored after 5 min of incubation with 10 mM DTT. These experiments indicate that *Tb*PTP1 is sensitive to reversible redox regulation, consistent with several characterized mammalian PTPs (Denu and Tanner, 1998).

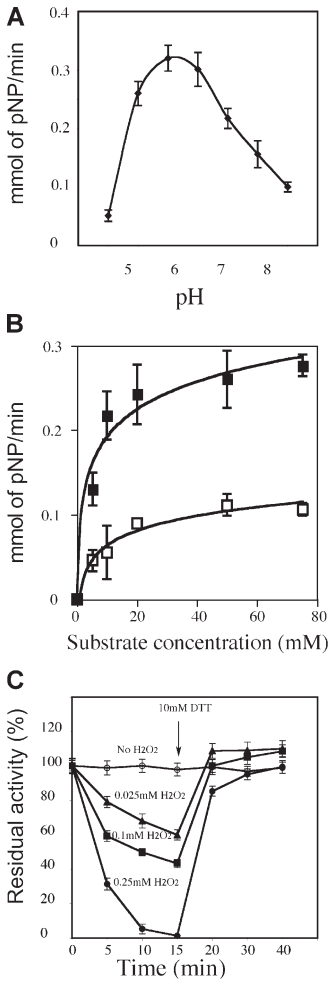

Figure 3. ***Tb*PTP1 activity is regulated by pH and redox.** (A) Activity profile of *Tb*PTP1 at different pH. (B) Effect of DTT on the specific activity of *Tb*PTP1. Activity was determined using various concentrations of pNPP with the assay buffer adjusted to pH 6.0. The assays were performed without DTT (open squares) or with 2 mM DTT (closed squares). (C) Reversible oxidation regulates *Tb*PTP1 activity. *Tb*PTP1 was inactivated with the addition of H_2O_2 and reactivated by the addition of DTT as reducing agent. *Tb*PTP1 was treated with various concentrations of H_2O_2: control/0 mM (open circles), 0.025 mM (closed triangles), 0.1 mM (closed squares), and 0.25 mM (closed circles). After the addition of H_2O_2, samples were tested for pNPP hydrolysis. After a 15-min incubation, 10 mM DTT was added to the samples to reactivate the oxidized-inactivated enzyme. The activity of the untreated enzyme is shown for comparison along the reduced/oxidized sample. All data points represent the means of triplicate determinations. Error bars indicate SEM. pNP, *p*-nitrophenol.

*Tb*PTP1 is a tyrosine-specific protein phosphatase

To test the specific activity of *Tb*PTP1, a full kinetic characterization of the wild-type enzyme was undertaken using a range of phosphorylated substrates. These included tyrosine-, serine-, and threonine-phosphorylated peptides; phospho–amino acids; nucleotides; phospholipids; and inorganic phosphorylated compounds (Fig. 4 A and Table S1). Most important, this analysis showed that *Tb*PTP1 favored tyrosine-phosphorylated substrates in the dephosphorylation assays while showing 10–40-fold less activity against the Ser/Thr-phosphorylated substrates. In contrast, *Tb*PTP1 exhibited little or no activity toward the phospholipids, nucleotides, or inorganic phosphocompounds tested, suggesting that the purified enzyme does not exhibit either lipid phosphatase or phosphoesterase activity. Analysis of the saturation kinetics of *Tb*PTP1 was also performed using the Tyr-phosphorylated EGF receptor peptide (pEGFR), the Insulin receptor peptide (pInsulin), phospho-Tyr (pTyr), and phospho-Ser (pSer). The results obtained showed that *Tb*PTP1 dephosphorylates the pEGFR peptide with the highest V_{max}, 1.5–2 times higher than for pInsulin peptide and pTyr, and six times higher than for pSer. As activity toward nucleotides, phospholipids, and inorganic phospocompounds was considerably lower or nonmeasurable, no further kinetic analysis was considered relevant for these compounds.

In a final series of biochemical experiments, the inhibitor profile of *Tb*PTP1 was investigated. The phosphatase activity of *Tb*PTP1 was assayed using pNPP or pEGFR peptide in the presence of different inhibitors. The PTP-specific inhibitor

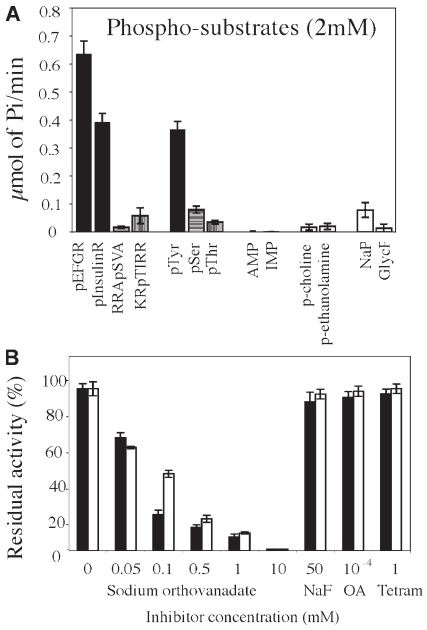

Figure 4. ***Tb*PTP1 shows a tyrosine-specific protein phosphatase activity and inhibitor profile.** (A) Various phosphosubstrates (2 mM final concentration) were assayed using a malachite green detection system. The tyrosine-phosphorylated EGFR (DADEpYLIPQQG) and insulin receptor (TRDIpYETDYYRK) were dephosphorylated with the highest rate followed by phosphoTyr amino acid. Other phosphosubstrates proved to be poor substrates for *Tb*PTP1. (B) Effect of various inhibitors on the activity of *Tb*PTP1. Concentrations and names of the inhibitors (OA, okadaic acid; Tetram, tetramisole) are indicated on the x axis. The fraction (%) of residual activities in the presence or in the absence of inhibitors is shown on the y axis. The filled columns show activity measured using pNPP as substrate, and the empty columns show the phosphatase assays performed using pEGFR as substrate. All data points represent the mean values of triplicate determinations, and error bars (± SEM) are indicated.

sodium orthovanadate impaired the catalytic activity of *Tb*PTP1 in a concentration-dependent manner (Fig. 4 B). Dephosphorylation of both pNPP and of the pEGFR peptide was reduced by 90% by 1 mM sodium orthovanadate, and the activity was completely abolished by 10 mM of this PTP inhibitor. In contrast, the Ser/Thr phosphatase inhibitor sodium fluoride had no measurable effect on the activity of *Tb*PTP1 toward either pNPP or pEGFR, even at concentrations of 50 mM. Likewise, no effect was observed with the PP1- and PP2A-specific inhibitor okadaic acid or with the alkaline phosphatase inhibitor tetramisole. Combined, these experiments confirmed our prediction, based on sequence analysis, that *Tb*PTP1 exhibits all the biochemical characteristics typical of a tyrosine-specific phosphatase.

*Tb*PTP1 ablation induces spontaneous differentiation to procyclic forms in a subset of bloodstream forms

To initiate a functional analysis in vivo, *Tb*PTP1 was targeted in cultured bloodstream forms by RNAi. The *Tb*PTP1 coding region was inserted into the vector pZJM (Wang et al., 2000) between two opposing T7 RNA polymerase promoters and transfected in to the "single marker" bloodstream line, which expresses T7 RNA polymerase (Wirtz et al., 1999). This results in *Tb*PTP1 double-stranded RNA expression, thereby invoking RNAi.

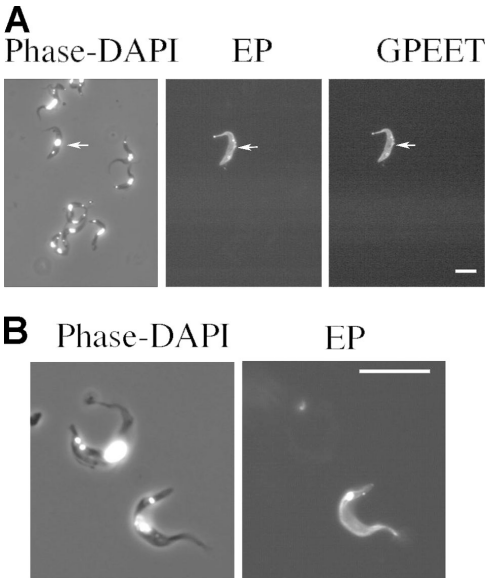

Figure 5. **RNAi for *Tb*PTP1 in bloodstream forms.** RNAi of *Tb*PTP 1 in *T. brucei* 427 single-marker bloodstream forms generates differentiated procyclic forms at 37°C in HMI-9. (A) A field with cells stained for EP or GPEET procyclin (arrows). (B) A cell where the kinetoplast is also positioned subterminally and there is EP procyclin staining. Bars, 15 μm.

We successfully generated several viable cell lines, although in only one case was effective ablation of *Tb*PTP1 mRNA and loss of protein observed, and this generated a subtle growth phenotype (Fig. S2, available at http://www.jcb.org/cgi/content/full/jcb.200605090/DC1). During phenotypic characterization of this cell line, we observed that a small proportion (2–12%) of cells spontaneously differentiated to procyclic forms despite maintenance of the cells in bloodstream form culture conditions (HMI-9 culture medium at 37°C). This phenotype manifested itself as the presence of cells in the population that stained strongly with antibodies specific for both EP and GPEET (Fig. 5 A) procyclin (Roditi and Clayton, 1999). Significantly, this did not represent loss of procyclin gene expression control alone (as can be observed at a frequency of up to 0.1% in wild-type bloodstream populations); analysis of the procyclin-stained cells indicated that they also exhibited characteristic procyclic-form morphology, with their mitochondrial genome (kinetoplast) being positioned away from the cell posterior (Matthews et al., 1995; Fig. 5 B). They also expressed the procyclic stage–specific cytoskeletal antigen CAP5.5 (Hertz-Fowler et al., 2001; unpublished data). Unfortunately, the differentiation phenotype was rapidly unstable and thus difficult to maintain in culture, with the proportion of differentiated cells decreasing in successive passages, even in the absence of induction.

The instability of the phenotype observed with *Tb*PTP1 RNAi prompted a search for alternative approaches to target the activity of this enzyme. Recently, a series of highly specific sulphonamido-benzabromarone allosteric inhibitors of PTP1B have been reported (Wiesmann et al., 2004), of which 3-(3,5-Dibromo-4-hydroxy-benzoyl)-2-ethyl-benzofuran-6-sulfonicacid-(4-(thiazol-2-ylsulfamyl)-phenyl)-amide (BZ3) exhibits good

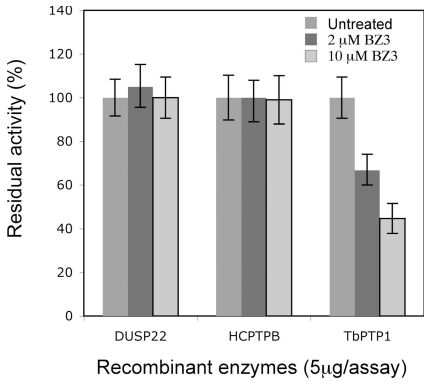

Figure 6. **BZ3 (0, 2, or 10 μM) inhibition of recombinant *Tb*PTP1, human low molecular weight phosphatase (HCPTPB), and a mammalian dual-specificity phosphatase.** In each case, pNPP was used as substrate. Error bars indicate SEM.

cell permeability. This compound prevents closure of the PTP1B WPD loop, thereby preventing dephosphorylation of substrates. To investigate whether this would provide a useful reagent for functional analysis of *Tb*PTP1, we tested the inhibition profile and specificity of BZ3 against *Tb*PTP1 and other PTPs. We found that 10 μM of BZ3 reduced the activity of *Tb*PTP1 at least 50%, consistent with its activity against human PTP1B (IC_{50} = 8 μM; Wiesmann et al., 2004), whereas a dual-specificity phosphatase and the human low molecular weight phosphatase HCPTPB, which lacks the WPD loop, showed no inhibition at this concentration (Fig. 6).

Having verified the specificity of BZ3 for *Tb*PTP1, we exposed monomorphic bloodstream forms in culture to a titration of BZ3 ranging from 50 to 150 μM, which was in the same range as the concentration effective against mammalian PTP1B in CHO cells in culture (250 μM; Wiesmann et al., 2004). Strikingly, this also resulted in spontaneous differentiation of a subset of the parasites in response to the inhibitor, with 150 μM BZ3 stimulating procyclin expression in the bloodstream population at a frequency of 9.4% (Table I). Moreover, the phenotype of the cells was consistent with that observed in the RNAi line; i.e., the procyclin expressers in the population also exhibited kinetoplast repositioning, indicative of morphological differentiation (unpublished data). In contrast, exposure of monomorphic bloodstream forms to a non–cell-permeable PTP inhibitor, sodium orthovanadate (at 1 mM), did not result

Table I. **Percentage of EP procyclin–positive cells in monomorphic cultures treated with phosphatase inhibitors**

Treatment	EP procyclin–positive cells
	%
Untreated monomorphic cells	0.3
+ DMSO	0
+ 50 μM BZ3	1.6
+ 100 μM BZ3	5.2
+ 150 μM BZ3	9.4
+ 1 mM NaOVanadate	0.6
+ 1 mM NaF	0.2

Cell samples were processed after 18 h under each condition.

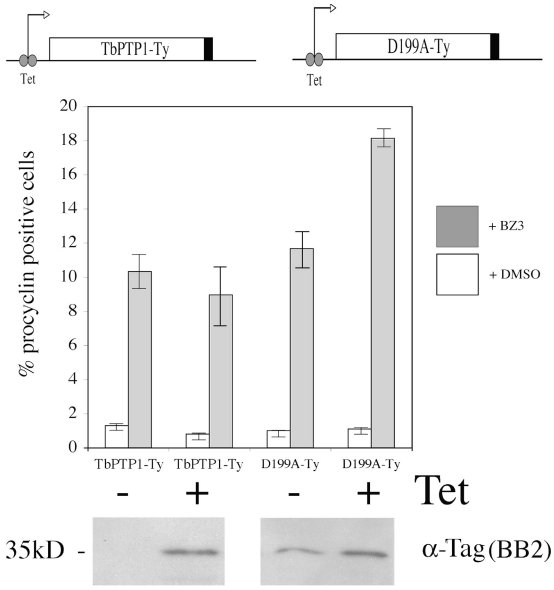

Figure 7. **BZ3 induced differentiation in bloodstream forms expressing wild-type *Tb*PTP1-Ty or the D199A *Tb*PTP1 mutant.** For each, transgene expression was induced (+Tet) or not (−Tet) for 3 d, with cells then being exposed to 150 μM BZ3. Expression of EP procyclin was assayed in 500 cells after 24 h. Induction of each ectopically expressed protein was verified by Western blotting using an antibody (BB2) directed against the Ty-1 epitope tag incorporated into each protein. The results of three independent experiments are shown, with error bars indicating the SEM. There was no difference in growth kinetics between each line before BZ3 addition (not depicted).

in detectable differentiation, nor did exposure to 1 mM NaF, a Ser/Thr phophatase inhibitor (Table I). Thus, *Tb*PTP1 inhibition promotes spontaneous differentiation to procyclic forms in the absence of exogenous trigger in a subset of bloodstream forms in culture.

To verify that *Tb*PTP1 was a target of BZ3 in vivo and that this was linked to the differentiation phenotype observed, transgenic bloodstream cells lines were generated which ectopically expressed wild type or a D199A mutant of *Tb*PTP1, which binds but not release substrates (Tonks, 2003), acting as a dominant-negative mutation (Fig. 7). When exposed to 150 μM BZ3, cells expressing the D199A mutant reproducibly exhibited significantly enhanced differentiation when compared with the same cell line in the absence of tetracycline induction (18.1% in the induced population versus 11.6% in the uninduced population; Tukey post hoc comparison, $P = 0.049$). In contrast, no enhanced differentiation was observed in cells that ectopically expressed the wild-type *Tb*PTP1 (9% in the induced population versus 10.3% in the uninduced population; $P = 0.86$). This demonstrates that expression of the D199A mutant of *Tb*PTP1 increases differentiation in response to BZ3. This provides further evidence that *Tb*PTP1 is a target of BZ3 in vivo and that this is linked to the observed differentiation phenotype.

BZ3 stimulates synchronous differentiation of stumpy forms

We wished to investigate why only a subset of monomorphic bloodstream trypanosomes underwent spontaneous differentiation

to procyclic forms when *Tb*PTP1 was inhibited. Monomorphic bloodstream forms are so named because they have lost the capacity to generate morphologically stumpy forms through prolonged laboratory passage. However, they do retain the capacity to differentiate to procyclic forms when stimulated with cis aconitate, although this is asynchronous in the population and of variable efficiency. We previously proposed that this asynchrony arises from the requirement for individual cells to undergo commitment to differentiation (Matthews and Gull, 1994; Tasker et al., 2000). These committed cells remain slender in morphology but are functionally equivalent to stumpy forms in terms of their ability to differentiate, a condition we have termed stumpy* (Tasker et al., 2000; Matthews et al., 2004). We hypothesized that the small proportion of monomorphic cells that differentiated in response to BZ3 or *Tb*PTP1 RNAi were these stumpy* forms, which was supported by the increased differentiation of these RNAi lines when incubated with a cAMP analogue reported to promote stumpy formation (Fig. S2 C). To further evaluate this, we investigated the response to BZ3 of homogenous populations of stumpy forms, which are uniformly and irreversibly committed to differentiation to procyclic forms. Our prediction was that these cells would show a highly efficient differentiation to procyclic forms in response to BZ3 when compared with cultured monomorphic lines.

Initially, we assayed BZ3-induced differentiation in pleomorphic slender cells derived from a rodent infection. This resulted in an ~7% differentiation after 24 h, consistent with the response of cultured monomorphic cells (Fig. S3, available at http://www.jcb.org/cgi/content/full/jcb.200605090/DC1). Thereafter, trypanosome populations highly enriched for stumpy forms were harvested from a mouse infection, and these cells were exposed either to 150 μM BZ3, 6 mM cis aconitate, or 0.3% vol/vol DMSO (used to solubilize BZ3). In all cases, the cells were then maintained in bloodstream-form culture conditions (37°C in HMI-9) over a period of 24 h, conditions that are compatible with both efficient differentiation of cis aconitate–stimulated cells (Matthews and Gull, 1997) and maintenance of the viability of undifferentiated stumpy forms. Samples were harvested at various time points and analyzed for the expression of EP procyclin by immunofluorescence and for morphological differentiation by quantitative analysis of the kinetoplast–posterior dimension in each cell population. Figs. 8 and 9 demonstrate the remarkable result of this analysis: stumpy populations differentiated to procyclic forms synchronously and efficiently when exposed to BZ3, with the kinetics of this being equivalent to cells exposed to cis aconitate (Matthews and Gull, 1994). Thus, by 6 h in 150 μM BZ3, >70% of cells were EP procyclin positive (Fig. 8 A), and by 24 h the kinetoplast–posterior dimension had increased from ~1 μm (equivalent to that seen in bloodstream forms) to ~5 μm (equivalent to that in procyclic forms; Matthews et al., 1995; Fig. 8 B). In contrast, cells exposed to DMSO alone remained as bloodstream stumpy forms and showed no evidence of differentiation to procyclic forms (Fig. 9 A). Moreover, by 24 h, differentiated cells in the 150 μM BZ3–treated population were undergoing cell division as differentiated procyclic forms and had induced expression of the procyclic stage–specific

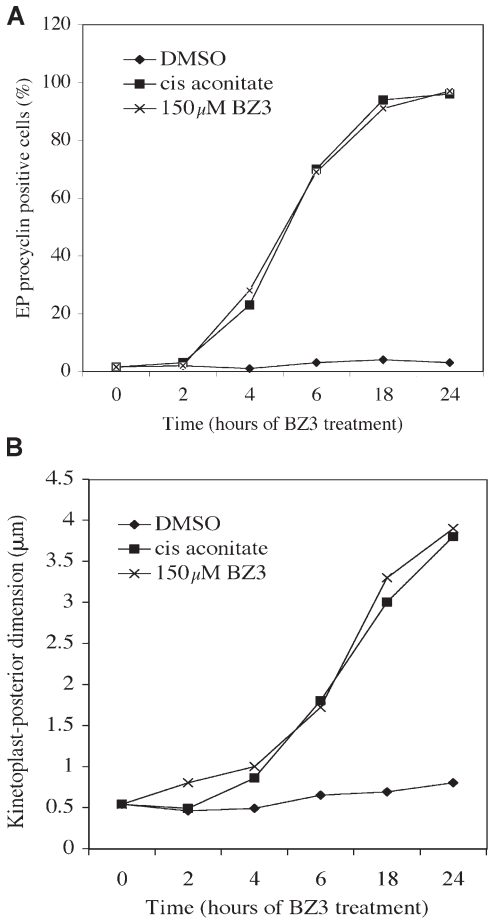

Figure 8. **BZ3 induces synchronous differentiation of stumpy forms.** (A) EP procyclin expression of stumpy forms after exposure to 6 mM cis aconitate, 150 μM BZ3, or 0.3% DMSO. (B) Kinetoplast–posterior distance (in μm) at each time point for cells under the different treatments. The values represent a mean of 100 individual cell measurements under each condition at each time point. Error bars indicate SEM.

cytoskeletal protein CAP5.5 (Matthews and Gull, 1994; Hertz-Fowler et al., 2001; Fig. 9, B and C). We conclude that inhibition of *Tb*PTP1 stimulates committed bloodstream-form trypanosomes to differentiate to procyclic forms in the absence of any previously described trigger for this process.

Discussion

In this study, we report the identification, biochemical characterization, and functional analysis of a novel *T. brucei* protein tyrosine phosphatase, *Tb*PTP1, implicated in life cycle differentiation control in *T. brucei*. *Tb*PTP1 was originally identified in a search for molecular markers of the nondividing bloodstream form of *T. brucei*, by analogy to other molecules associated with G0 arrest in eukaryotic cells. Bioinformatics analysis of the *Tb*PTP1 sequence and further searches in other kinetoplastid genomes revealed the existence of orthologue protein tyrosine phosphatases in the other trypanosomatids *T. vivax*, *T. congolense*, and *T. cruzi*. All of them contain the well-defined motifs conserved in classical PTPs, necessary for catalysis and substrate binding. In addition, distinct motifs are conserved in the

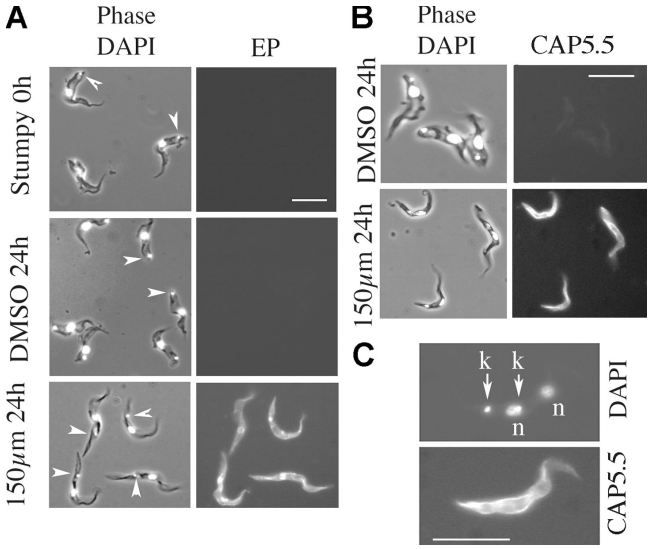

Figure 9. **The differentiation phenotype of BZ3-treated stumpy forms.** (A) EP procyclin expression and kinetoplast position of stumpy form cells at either 0 or 24 h after exposure to DMSO or 150 μM BZ3. (left) Phase-contrast DAPI-stained images are shown. The kinetoplast position is marked with an arrowhead in example cells. Note that repositioning of kinetoplast with respect to the cell posterior end occurred only in cells treated with 150 μM BZ3. (right) The same cells are stained for EP procyclin. (B) Cells were treated either with DMSO or 150 μM BZ3 for 24 h and stained with CAP5.5. (C) A cell that is undergoing cell division and expresses CAP5.5 is shown. This indicates cell cycle reentry for the differentiated cells. k, segregated kinetoplasts; n, postmitotic nuclei. Bars, 15 μm.

trypanosomal subfamily of phosphatases, both in the catalytic region and in the N-terminal region, upstream of the catalytic domain. We suggest that these *Trypanosoma* spp.–specific motifs could be important in functional regulation of *Tb*PTP1.

When expressed as a recombinant protein, *Tb*PTP1 preferentially dephosphorylated phosphotyrosine substrates and was inhibited in vitro by sodium orthovanadate, a known tyrosine-specific phosphatase inhibitor. Moreover, the enzyme was regulated by reversible oxidation and mutation of the predicted essential catalytic residues C229 and D199 resulted in proteins with either severely impaired enzymatic activity (D199A) or total inactivity (C229S). Together, these results confirm the assignment of *Tb*PTP1 as a phosphotyrosine-specific phosphatase. This contrasts with previously reported phosphatases in *T. brucei*, for which our sequence analysis failed to find any of the conserved PTP-specific motifs or any homology to the classical PTPs (Bakalara et al., 2000). Thus, *Tb*PTP1 is to our knowledge the first report of a cloned gene encoding a bona fide nonreceptor tyrosine-specific phosphatase in these organisms.

The biological function of *Tb*PTP1 was investigated by two experimental approaches: gene-specific RNAi and using a cell-permeable PTP1B-specific inhibitor in vivo. The first approach implicated *Tb*PTP1 in life cycle regulation, with spontaneous differentiation being observed in a subset of cultured bloodstream-form cells. However, this phenotype was unstable, and the proportion of differentiated cells was reduced to wild-type levels with continued culture of the parasites whether cells were induced or not. This is not surprising, as transfection procedures and continued passage at 37°C in bloodstream-specific culture media would quickly select against populations that generate procyclic forms. Moreover, other functions of *Tb*PTP1 in proliferative bloodstream forms cannot be excluded. Therefore, we also analyzed the effect of a recently characterized cell-permeable allosteric inhibitor of PTP1B, a benzabromarone derivative (Wiesmann et al., 2004). This inhibitor prevents the closure of the WPD loop of PTPs, therefore keeping the enzyme in a catalytically inactive form. We demonstrated that this inhibitor was effective against *Tb*PTP1, but not against the human low molecular weight PTP (LMWPTP) or a dual-specificity phosphatase. Analysis of the phosphatase complement of the complete *T. brucei* genome identified only two putative proteins with an intact WPD loop motif and predicted tyrosine phosphatase activity. One of these is *Tb*PTP1, and we have confirmed its BZ3 sensitivity here. The second enzyme, which we term *Tb*PTP2 (Tb11.01.5450), is not likely to contribute to the observed differentiation phenotype, as RNAi against this enzyme does not elicit differentiation of bloodstream forms (unpublished data). Although we cannot exclude other potential uncharacterized targets in trypanosomes, the compatible phenotypes resulting from genetic and pharmacological inhibition of *Tb*PTP1 implicate this enzyme as being responsible for the differentiation phenotype. Moreover, specificity of the response was further supported by the enhanced differentiation observed in BZ3-treated cells expressing the dominant-negative D199A mutant of *Tb*PTP1.

Only a small subset of bloodstream-form cells in asynchronous in vitro cultures were stimulated to differentiate to procyclic forms by BZ3. However, the most striking observation was the effect of this inhibitor on uniform populations of stumpy forms. Here, treatment with the PTP1B inhibitor resulted in efficient differentiation to procyclic forms. We observed that stage-regulated protein expression (EP procyclin; CAP5.5), kinetoplast repositioning, and cell cycle progression all occurred with equivalent efficiency and on the same time scale as cells treated with cis aconitate, an established trigger for trypanosome differentiation. We interpret the differentiation of the small proportion of cells in bloodstream cultures as the response of the subset of cells in this population, which have entered division arrest or committed to other early events in stumpy formation, before morphological transformation. We previously referred to these cells as stumpy* forms (Tasker et al., 2000).

In Fig. 10, we present a model for the role of *Tb*PTP1 in the control of bloodstream to procyclic differentiation. In this model, bloodstream parasites commit to stumpy formation and become competent (stumpy*) to differentiate to procyclic forms. However, they are held arrested in this state in the bloodstream by the action of *Tb*PTP1. Then, upon uptake by the tsetse fly, this inhibition is removed and the parasites progress unhindered to procyclic forms, progressing through a highly programmed developmental pathway in which cellular events occur on a predetermined pathway and time scale. This model has two important implications. First, it supports the concept that proliferative slender cells are not competent to differentiate to procyclic forms unless they commit to the early events of stumpy formation, in particular, cell cycle arrest. Also, it

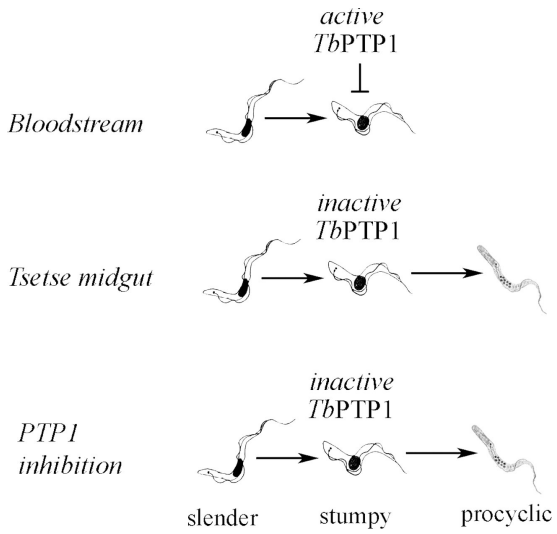

Figure 10. **A model for the control of bloodstream to procyclic form differentiation in trypanosomes.** In the bloodstream, slender forms transform to stumpy forms and then stay arrested, with further differentiation being inhibited by the action of *Tb*PTP1. Once in the tsetse midgut, inhibition of stumpy form differentiation is released and procyclic forms are generated. Inactivation of *Tb*PTP1 function by RNAi or treatment with the BZ3 inhibitor mimics the release of differentiation blockage observed in the natural life cycle and results in direct differentiation of stumpy forms to procyclic forms, despite the absence of other differentiation stimuli.

suggests that the default pathway for stumpy forms is to differentiate directly to procyclic forms and that this differentiation is inhibited in the bloodstream by the action of *Tb*PTP1. In other words, differentiation primarily results from release of the "brake," rather than application of the "accelerator." This scenario is compatible with the role of PTP1 in *Dictyostelium* slug development, where removal of a PTP1 precipitates accelerated differentiation via cell aggregation (Howard et al., 1992).

This model does not predict what is the natural signal that triggers the inactivation of *Tb*PTP1, although one possibility is the different conditions to which the trypanosome is exposed upon entering the fly. For example, pH fluctuations have been observed in the tsetse digestive tract from pH 9.0 to pH 10.2 (Liniger et al., 2003), at which the activity of *Tb*PTP1 is considerably lower. Potentially combined with other specific signals, for example, changes in redox conditions upon tsetse uptake, this would then inactivate *Tb*PTP1 and license the trypanosome for cell cycle reentry and differentiation into a proliferative procyclic form.

The proposed role of *Tb*PTP1 in preventing inappropriate differentiation of stumpy forms in the mammalian bloodstream is essential for transmissibility of the parasite. If not strictly controlled, the progression to procyclic forms would result in rapid death of the stumpy population in the bloodstream because of either the activation of complement by the alternative pathway (killing cells that have lost the variant surface glycoprotein) or the generation of antibodies to invariant procyclic surface antigens. This makes *Tb*PTP1 a key component of the regulation of the trypanosome life cycle and hence a potentially important pharmacological target for controlling trypanosome transmission, for example, in epidemic foci involving intensive human–human or human–livestock transmission. If coupled with factors to promote stumpy formation, targeting *Tb*PTP1 may also help limit parasite virulence and promote trypanosome clearance. There is intense interest in the development of PTP1B inhibitors in the pharmaceutical industry because of the importance of these enzymes in diabetes and obesity (Ukkola and Santaniemi, 2002; Zhang and Lee, 2003), and we are currently investigating the opportunity for piggyback strategies to target kinetoplastid PTPs. Significantly, the presence of trypanosome-specific motifs in this enzyme offers the potential for developing inhibitors with specificity for the parasite enzyme with respect to their mammalian counterparts.

Materials and methods

Materials

Phosphosubstrates and other chemicals were purchased from Sigma-Aldrich. The Threonine (KRpTIRR) and Serine (RRApSVA) phosphopeptides were obtained from Upstate. The PTP1B inhibitor BZ3 was purchased from Calbiochem.

Parasite growth and differentiation

Parasite lines used were *T.b. rhodesiense* EATRO 2340 GUP2965 (monomorphic slender forms) or, for stumpy generation, the isogenic pleomorphic line GUP2962 (Matthews and Gull, 1994). For RNAi analyses, *T.b. brucei* Lister 427 single-marker cells were used (a gift from G. Cross, Rockefeller University, New York, NY; Wirtz et al., 1999), whereas established procyclic forms were *T.b. brucei* Lister 427.

For BZ3 inhibition assays, cells in HMI-9 medium (Hirumi and Hirumi, 1989) at 37°C were exposed to DMSO, PTP1B inhibitor BZ3, or 6 mM cis aconitate. Samples were assayed by immunofluorescence at room temperature using antibody to EP procyclin (diluted 1:500 in PBS; Cedar Lane Laboratories), antibody to GPEET (diluted 1:200; a gift from I. Roditi, University of Bern, Bern, Switzerland), or the procyclic form cytoskeletal protein CAP5.5 (undiluted hybridoma supernatant; a gift from K. Gull, University of Oxford, Oxford, England; Hertz-Fowler et al., 2001). Secondary antibodies used were goat anti–mouse (EP procyclin; CAP5.5) or –rabbit (GPEET procyclin) conjugated to either FITC (1:50; Sigma-Aldrich) or Alexa 488 (1:200; Invitrogen). Slides were stained with 1 μg/ml DAPI and mounted in MOWIOL (Harlow Chemical Co.). Morphometric measurements of kinetoplast repositioning used Scion Image 1.62. Images were captured using a Cohu charged-coupled device camera attached to an Axioscope 2 (Carl Zeiss MicroImaging, Inc.) using either Plan Neofluar 63× (1.25 NA) or Plan Neofluar 100× (1.30 NA) phase-contrast objectives. Images were processed using Photoshop CS (Adobe).

DNA cloning

A 595-bp fragment related to PTPROt (Aguiar et al., 1999) formed part of the sheared *T. brucei* strain TREU 927/4 genomic DNA clone 18E19 (available from GenBank/EMBL/DDBJ under accession no. AQ649023). Oligonucleotides were designed to the 5′ (*Tb*PTP A; 5′-CATCAACCTCGTACGACG-3′) and 3′ (*Tb*PTP B; 5′-CAAGCCATACAATAATTG-3′) ends of the gene fragment, and were these used in independent amplifications with primers specific for the spliced leader sequence or polyA tail to amplify the gene in two overlapping halves from cDNA. The sequence of the full gene was verified after completion of the trypanosome genome sequence.

Northern and Western blotting

RNA preparation and Northern blotting was performed as described by Tasker et al. (2000) using a digoxygenin-labeled *Tb*PTP1-specific riboprobe (Roche). Stumpy cell fractionation used the Qproteome kit (QIAGEN) with each fraction being probed with antibodies to α-tubulin (cytoskeletal fraction; a gift from K. Gull), cytosolic PGK (cytosol; a gift from P. Michels, Université Catholique de Louvain, Brussels, Belgium), and BiP (membrane and organelles; a gift from J. Bangs, University of Wisconsin, Madison, WI) as controls. For detection of *Tb*PTP1, an anti-peptide (NH_2-AMKQKRFGMVQRLEQ-COOH) antibody was raised in rabbits and affinity purified against the immunogen (Eurogentec). Preimmune serum detected no trypanosome protein. Western blotting was performed according to Tasker et al. (2000).

RNAi and ectopic expression for *Tb*PTP1 and mutants

*Tb*PTP1 transcript ablation in bloodstream forms was achieved by cloning the *Tb*PTP1 coding sequence into pZJM (Wang et al., 2000), which was then linearized by NotI digestion and transfected as previously described. Transformants were selected with 2.5 μg/ml phleomycin. Ectopic overexpression of *Tb*PTP1 and D199A mutants used the trypanosome expression vector pHD451.

Phosphatase assays using phosphosubstrates

Dephosphorylation of phosphosubstrates was detected by measuring the release of inorganic phosphate with the malachite green detection system according to the manufacturer's protocol (Protein tyrosine phosphatase assay kit; Sigma-Aldrich). Reaction mixtures (50 μl) contained 5–10 μg of purified *Tb*PTP1 with concentrations from 0.01 to 0.2 mM of phosphopeptides in 50 mM Hepes and 150 mM NaCl, pH 7.0. Reactions were incubated at 37°C for 15–30 min and quenched by adding of 50 μl of malachite green reagent. After 15 min of further incubation at room temperature, the absorbance of the samples were measured at 620 nm in a microplate reader (Opsys MR; Dynex Technologies), with released inorganic phosphate being determined using a phosphate standard curve. The specific activity is defined as pmoles of inorganic phosphate released in a minute per milligram of protein. Kinetic constants K_m and V_{max} were calculated using the Lineweaver-Burke plot of the reciprocal initial velocity versus the reciprocal concentration of substrates. See the supplemental text (available at http://www.jcb.org/cgi/content/full/jcb.200605090/DC1) for information about protein expression constructs and recombinant protein purification.

Phosphatase assays using pNPP

Enzyme activity was measured by monitoring *Tb*PTP1 (5–20 μg) catalyzed hydrolysis of pNPP to *p*-nitrophenol (Zhang and Van Etten, 1990). A final concentration of 20 mM pNPP was present in the assay. The pNPP assay buffer was 50 mM Tris, 50 mM bisTris, and 100 mM Na acetate, pH 5–7.5. Each reaction (400 μl) was performed in triplicate, being incubated at 37°C for 15 min and quenched by adding 500 μl of 1 M NaOH. The concentration of released *p*-nitrophenol, determined at 405 nm, was converted to millimolar units using a millimolar extinction coefficient of 18.0 mM^{-1} cm^{-1}.

Reversible inactivation of *Tb*PTP1 by H_2O_2

The assays (120 μl) contained 60 μg of *Tb*PTP1 and 0–0.25 mM H_2O_2 in 50 mM Hepes, pH 7.0, and 150 mM NaCl. Reactions, initiated by addition of H_2O_2, were incubated at room temperature. After 15 min, 10 mM DTT was added. 20-μl samples removed at 0, 5, 10, 15, 20, 30, and 40 min were assayed for residual activity using pNPP as substrate.

Online supplemental material

Table S1 shows kinetic constants for the hydrolysis of phosphosubstrates by *Tb*PTP1. Fig. S1 shows immunofluorescence localization of ectopically expressed *Tb*PTP1. Fig. S2 shows growth kinetics, RNA, and protein expression of the *Tb*PTP1 RNAi line and the response of the *Tb*PTP RNAi line to pCPTcAMP. Fig. S3 shows BZ3 response of pleomorphic slender cells. Online supplemental material is available at http://www.jcb.org/cgi/content/full/jcb.200605090/DC1.

We thank Humera Tariq and Pablo Rios for the gift of recombinant phosphatases, Dr. Hui Lu for assistance, and Professor Victor Rodwell for reviewing the manuscript. We also thank Professors Jay Bangs, Keith Gull, Isabel Roditi, and Paul Michels for the gift of antibodies and Dr. Nick Colgrave for statistical analyses.

This work was supported by Wellcome Trust grant 068793 and by Wellcome Trust Programme grant 073358 to K.R. Matthews.

Submitted: 15 May 2006
Accepted: 19 September 2006

References

Aguiar, R.C., Y. Yakushijin, S. Kharbanda, S. Tiwari, G.J. Freeman, and M.A. Shipp. 1999. PTPROt: an alternatively spliced and developmentally regulated B-lymphoid phosphatase that promotes G0/G1 arrest. *Blood.* 94:2403–2413.

Andersen, J.N., O.H. Mortensen, G.H. Peters, P.G. Drake, L.F. Iversen, O.H. Olsen, P.G. Jansen, H.S. Andersen, N.K. Tonks, and N.P. Moller. 2001. Structural and evolutionary relationships among protein tyrosine phosphatase domains. *Mol. Cell. Biol.* 21:7117–7136.

Bakalara, N., A. Seyfang, T. Baltz, and C. Davis. 1995a. *Trypanosoma brucei* and *Trypanosoma cruzi*: life cycle-regulated protein tyrosine phosphatase activity. *Exp. Parasitol.* 81:302–312.

Bakalara, N., A. Seyfang, C. Davis, and T. Baltz. 1995b. Characterization of a life-cycle-stage-regulated membrane protein tyrosine phosphatase in *Trypanosoma brucei*. *Eur. J. Biochem.* 234:871–877.

Bakalara, N., X. Santarelli, C. Davis, and T. Baltz. 2000. Purification, cloning, and characterization of an acidic ectoprotein phosphatase differentially expressed in the infectious bloodstream form of *Trypanosoma brucei*. *J. Biol. Chem.* 275:8863–8871.

Barrett, M.P., R.J. Burchmore, A. Stich, J.O. Lazzari, A.C. Frasch, J.J. Cazzulo, and S. Krishna. 2003. The trypanosomiases. *Lancet.* 362:1469–1480.

Black, D.S., A. Marie-Cardine, B. Schraven, and J.B. Bliska. 2000. The *Yersinia* tyrosine phosphatase YopH targets a novel adhesion-regulated signalling complex in macrophages. *Cell. Microbiol.* 2:401–414.

Cool, D.E., and J.J. Blum. 1993. Protein tyrosine phosphatase activity in *Leishmania donovani*. *Mol. Cell. Biochem.* 127-128:143–149.

Denu, J.M., and K.G. Tanner. 1998. Specific and reversible inactivation of protein tyrosine phosphatases by hydrogen peroxide: evidence for a sulfenic acid intermediate and implications for redox regulation. *Biochemistry.* 37:5633–5642.

Engstler, M., and M. Boshart. 2004. Cold shock and regulation of surface protein trafficking convey sensitization to inducers of stage differentiation in *Trypanosoma brucei*. *Genes Dev.* 18:2798–2811.

Hertz-Fowler, C., K. Ersfeld, and K. Gull. 2001. CAP5.5, a life-cycle-regulated, cytoskeleton-associated protein is a member of a novel family of calpain-related proteins in *Trypanosoma brucei*. *Mol. Biochem. Parasitol.* 116:25–34.

Hirumi, H., and K. Hirumi. 1989. Continuous cultivation of *Trypanosoma brucei* blood stream forms in a medium containing a low concentration of serum protein without feeder cell layers. *J. Parasitol.* 75:985–989.

Howard, P.K., B.M. Sefton, and R.A. Firtel. 1992. Analysis of a spatially regulated phosphotyrosine phosphatase identifies tyrosine phosphorylation as a key regulatory pathway in *Dictyostelium*. *Cell.* 71:637–647.

Howard, P.K., B.M. Sefton, and R.A. Firtel. 1993. Tyrosine phosphorylation of actin in *Dictyostelium* associated with cell-shape changes. *Science*. 259:241–244.

Lin, S.L., T.X. Le, and D.S. Cowen. 2003. SptP, a *Salmonella typhimurium* type III-secreted protein, inhibits the mitogen-activated protein kinase pathway by inhibiting Raf activation. *Cell. Microbiol.* 5:267–275.

Liniger, M., A. Acosta-Serrano, J. Van Den Abbeele, C. Kunz Renggli, R. Brun, P.T. Englund, and I. Roditi. 2003. Cleavage of trypanosome surface glycoproteins by alkaline trypsin-like enzyme(s) in the midgut of *Glossina morsitans*. *Int. J. Parasitol.* 33:1319–1328.

Matthews, K.R. 2005. The developmental cell biology of *Trypanosoma brucei*. *J. Cell Sci.* 118:283–290.

Matthews, K.R., and K. Gull. 1994. Evidence for an interplay between cell cycle progression and the initiation of differentiation between life cycle forms of African trypanosomes. *J. Cell Biol.* 125:1147–1156.

Matthews, K.R., and K. Gull. 1997. Commitment to differentiation and cell cycle re-entry are coincident but separable events in the transformation of African trypanosomes from their bloodstream to their insect form. *J. Cell Sci.* 110:2609–2618.

Matthews, K.R., T. Sherwin, and K. Gull. 1995. Mitochondrial genome repositioning during the differentiation of the African trypanosome between life cycle forms is microtubule mediated. *J. Cell Sci.* 108:2231–2239.

Matthews, K.R., J.R. Ellis, and A. Paterou. 2004. Molecular regulation of the life cycle of African trypanosomes. *Trends Parasitol.* 20:40–47.

Nascimento, M., N. Abourjeily, A. Ghosh, W.W. Zhang, and G. Matlashewski. 2003. Heterologous expression of a mammalian protein tyrosine phosphatase gene in *Leishmania*: effect on differentiation. *Mol. Microbiol.* 50:1517–1526.

Neel, B.G., and N.K. Tonks. 1997. Protein tyrosine phosphatases in signal transduction. *Curr. Opin. Cell Biol.* 9:193–204.

Nolan, D.P., S. Rolin, J.R. Rodriguez, J. Van Den Abbeele, and E. Pays. 2000. Slender and stumpy bloodstream forms of *Trypanosoma brucei* display a differential response to extracellular acidic and proteolytic stress. *Eur. J. Biochem.* 267:18–27.

Parsons, M., M. Valentine, J. Deans, G.L. Schieven, and J.A. Ledbetter. 1991. Distinct patterns of tyrosine phosphorylation during the life cycle of *Trypanosoma brucei*. *Mol. Biochem. Parasitol.* 45:241–248.

Parsons, M., E.A. Worthey, P.N. Ward, and J.C. Mottram. 2005. Comparative analysis of the kinomes of three pathogenic trypanosomatids: *Leishmania major*, *Trypanosoma brucei* and *Trypanosoma cruzi*. *BMC Genomics.* 6:127.

Roditi, I., and C. Clayton. 1999. An unambiguous nomenclature for the major surface glycoproteins of the procyclic form of *Trypanosoma brucei*. *Mol. Biochem. Parasitol.* 103:99–100.

Salmeen, A., J.N. Andersen, M.P. Myers, T.C. Meng, J.A. Hinks, N.K. Tonks, and D. Barford. 2003. Redox regulation of protein tyrosine phosphatase 1B involves a sulphenyl-amide intermediate. *Nature.* 423:769–773.

Sbicego, S., E. Vassella, U. Kurath, B. Blum, and I. Roditi. 1999. The use of transgenic *Trypanosoma brucei* to identify compounds inducing the differentiation of bloodstream forms to procyclic forms. *Mol. Biochem. Parasitol.* 104:311–322.

Singh, R., V. Rao, H. Shakila, R. Gupta, A. Khera, N. Dhar, A. Singh, A. Koul, Y. Singh, M. Naseema, et al. 2003. Disruption of mptpB impairs the ability of *Mycobacterium tuberculosis* to survive in guinea pigs. *Mol. Microbiol.* 50:751–762.

Tasker, M., J. Wilson, M. Sarkar, E. Hendriks, and K. Matthews. 2000. A novel selection regime for differentiation defects demonstrates an essential role for the stumpy form in the life cycle of the African trypanosome. *Mol. Biol. Cell.* 11:1905–1917.

Thompson, J.D., T.J. Gibson, F. Plewniak, F. Jeanmougin, and D.G. Higgins. 1997. The CLUSTAL_X windows interface: flexible strategies for multiple sequence alignment aided by quality analysis tools. *Nucleic Acids Res.* 25:4876–4882.

Tonks, N.K. 2003. PTP1B: from the sidelines to the front lines! *FEBS Lett.* 546:140–148.

Turner, C.M., N. Aslam, and C. Dye. 1995. Replication, differentiation, growth and the virulence of *Trypanosoma brucei* infections. *Parasitology.* 111:289–300.

Ukkola, O., and M. Santaniemi. 2002. Protein tyrosine phosphatase 1B: a new target for the treatment of obesity and associated co-morbidities. *J. Intern. Med.* 251:467–475.

van Ham, M., L. Kemperman, M. Wijers, J. Fransen, and W. Hendriks. 2005. Subcellular localization and differentiation-induced redistribution of the protein tyrosine phosphatase PTP-BL in neuroblastoma cells. *Cell. Mol. Neurobiol.* 25:1225–1244.

van Montfort, R.L., M. Congreve, D. Tisi, R. Carr, and H. Jhoti. 2003. Oxidation state of the active-site cysteine in protein tyrosine phosphatase 1B. *Nature.* 423:773–777.

Vassella, E., B. Reuner, B. Yutzy, and M. Boshart. 1997. Differentiation of African trypanosomes is controlled by a density sensing mechanism which signals cell cycle arrest via the cAMP pathway. *J. Cell Sci.* 110:2661–2671.

Wang, Z., J.C. Morris, M.E. Drew, and P.T. Englund. 2000. Inhibition of *Trypanosoma brucei* gene expression by RNA interference using an integratable vector with opposing T7 promoters. *J. Biol. Chem.* 275:40174–40179.

Wiesmann, C., K.J. Barr, J. Kung, J. Zhu, D.A. Erlanson, W. Shen, B.J. Fahr, M. Zhong, L. Taylor, M. Randal, et al. 2004. Allosteric inhibition of protein tyrosine phosphatase 1B. *Nat. Struct. Mol. Biol.* 11:730–737.

Wirtz, E., S. Leal, C. Ochatt, and G.A. Cross. 1999. A tightly regulated inducible expression system for conditional gene knock-outs and dominant-negative genetics in *Trypanosoma brucei*. *Mol. Biochem. Parasitol.* 99:89–101.

Zhang, Z.Y., and R.L. Van Etten. 1990. Purification and characterization of a low-molecular-weight acid phosphatase–a phosphotyrosyl-protein phosphatase from bovine heart. *Arch. Biochem. Biophys.* 282:39–49.

Zhang, Z.Y., and S.Y. Lee. 2003. PTP1B inhibitors as potential therapeutics in the treatment of type 2 diabetes and obesity. *Expert Opin. Investig. Drugs.* 12:223–233.

Ziegelbauer, K., and P. Overath. 1990. Surface antigen change during differentiation of *Trypanosoma brucei*. *Biochem. Soc. Trans.* 18:731–733.